DESIGN OF A HYDRAULIC MOTION CONTROL SYSTEM USING TWO BACKSTEPPING TIME VARYING SLIDING MODE STRATEGIES

Aws M. Abdullah[1], Shibly A. Al – Samarraie[2], Hasan H. Ali[3], Arif A. Al-Qassar[4]
[1]University of Baghdad, Baghdad, Iraq
[2]Control and Systems Engineering Department, University of Technology, Baghdad, Iraq
[3]Directorate of Studies, Planning, and Follow-up, Ministry of Higher Education and Scientific Research, Baghdad, Iraq
[4]Control and Systems Engineering Department, University of Technology, Baghdad, Iraq
**corresponding author: Aws M. Abdullah*
Email: aws.abd@cois.uobaghdad.edu.iq

Abstract - A second-order sliding mode control is used for high-order uncertain plants using equivalent control approach to improve the performance of control systems. They combine backstepping with quasi-continuous controller and twisting controllers. This paper considers a two of the most popular controllers that are used to solve the nonlinearities problem which are the backstepping quasi-continuous control (BQCC) and backstepping twisting controllers to control the angular velocity of a hydraulic motor to improve tracking performance and robustness to uncertainties. For the system dynamics, a linear state feedback with suitable high gain was designed as the virtual controller, where steady state error can be made arbitrarily small according to the gain value. A time varying sliding variable was then selected based on the designed virtual controller. The main benefit of using time varying sliding variable is that the system torque required is initially zero, in addition to the fact that its increasing rate can be put in a suitable range. The system's stability analysis has been presented using the Lyapunov function in the low level subsystem. The second order control action was used for the high level subsystem and the conventional sliding mode is used for the low level subsystem. The performance and the robustness of the proposed control in forcing the angular velocity to track the reference value (**100-2000 *RPM***) with uncertainty of (**±10%**) and disturbances of (**5-30 *N.m***) in the system parameters were studied. First, the mathematical model of the system was created. Then, Matlab-based simulation was used to assess the system performance. The results showed that the system exhibits excellent performance and robustness for multi-step input and multiplicative uncertainty.

Keywords: Inlet throttling velocity control system, Robust control, Sliding mode control, Uncertainty.

1. Introduction

The hydrostatic transmission systems are widely used in many applications because the system has high efficiency of the primary power source, the system is highly efficient even under partial load. Furthermore, high power-to-weight ratios, fast and smooth response characteristics and low cost in comparison to other types of drives. The hydrostatic transmission systems have some problems in controlling of the angular velocity for the rotary actuator, mainly because of the uncertainties in the parameters. This proposed hydrostatic transmission system consists mainly of the inlet-throttled pump, a throttling valve for adjusting the pump flow rate, and a rotary actuator, as shown in Figure 1.

The proposed system regulates the volume of fluid flow, which determines the velocity of the actuator [1,2].

The inlet throttled system combines the advantages of pump control systems and valve control systems in terms of simplicity, cost and efficiency. Table 1 gives a definition of system model.

The Quasi-Continuous and Twisting are 2-Sliding Mode Controllers, they are used with systems in presence of the disturbances and the variation in their parameters. Backstepping control design is used for designing the Quasi-Continuous and Twisting Controllers. Lyapunov functions are used as guides to ensure stability at lower level subsystem, [3].

Table (1): A definition of system model

Symbol	Quantity
P_A	Fluid pressures on the input of the actuator
P_B	Fluid pressures output of the actuator
V_a	Volumetric displacement of The actuator per unit of rotation
η_{at}	Actuator Torque Efficiency
J	mass moment of inertia
b	Viscous Damping Coefficient
θ	angular displacement
$\dot{\theta}$	angular velocity
$\ddot{\theta}$	angular acceleration
V	instantaneous volume of the chamber
V_O	Volume of the chamber when θ equals zero
β	Fluid bulk modulus of elasticity
Q_i	Volumetric flow rate from the charge pump
k_1	Coefficient of leakage
k_s	Valve Static Gain
t_d	Valve Time Delay
ω_n	Valve Natural Frequency
k_v	Constant of proportionality
A_v	Valve openning area
T_d	Disturbance Torque

Numerous studies investigated the use of the sliding mode controller to the hydraulic systems, a novel Adaptive-Gain Twisting controller (ATC) algorithm that is robust to the bounded disturbances with the unknown boundaries is proposed in [4]. The efficiency of the proposed (ATC) is experimentally verified on a mass–spring–damper system, with the reduction in control chattering. A novel finite time convergent output feedback adaptive-gain twisting controller with adaptive super-twisting observer in the feedback path is proposed in [5]. The efficacy of the proposed scheme is improved in the system. Variable Gain Super-Twisting Algorithm (VGSTA) is proposed in [6]. The effectiveness of the proposed design procedures was validated through experimental results. Many methods had been proposed for instance, some principal SMCs with their relative sliding surfaces and Lyapunov functions were illustrated in [7]. Dozens of articles have applied SMC to UAVs in order to solve the position and the attitude tracking problems ensuring robustness against external disturbances. An algorithm based on a higher order sliding mode control (HOSMC) technique, known as super-twisting algorithm, was used in [8] and in [9]. Second order sliding mode controller was also proposed in [10], and [11] used a HOSM observer as an estimator of the effect of the external disturbances such as wind and noise. Integral sliding mode controller was proposed in [12], and an adaptive sliding mode controller was developed in [13].

In this work, the flow rate is controlled by the inlet throttling valve and a fixed displacement pump. This system is characterized by its low cost and high efficiency. However, controlling the motion of the system is challenging due to the nonlinearities and uncertainties associated with the system. The stability and performance of the closed-loop situations were studied. The main purpose of this paper is to design a robust controller to the model system in spite of the variation in parameters values. A Backstepping Quasi-Continuous and Backstepping Twisting Controllers for closed-loop operation are utilized here to direct the actuator speed to the desired value with considering to parameters variation. The numerical simulations will demonstrate the effectiveness of the proposed controllers with a broad range of the parameters variation. The multiplicative parametric uncertainty was studied, and the system's robustness was evaluated with six of the parameters are related to the valve dynamics which are the natural frequency, the damping ratio, the static gain, and the time delay, the other two parameters are the discharge coefficient and the fluid bulk modulus. All these parameter changes were considered within the range of (+/−) 10% of their nominal values.

The present work organized as follows: firstly, it is introduced an overview to the second order sliding mode control and backstepping. Secondly, the model of the hydraulic system is presented in next section. After that the required steps and assumptions for designing a Quasi-Continuous and Twisting controllers are introduced, the numerical results of the effectiveness of the proposed controllers with comparisons between them and the conclusions are presented in the latter sections.

2. System Description

As shown in Figure 1, the proposed hydrostatic transmission system utilizes inlet throttling valve for controlling the flow. Fixed displacement pump is utilized for pumping the flow during a desired pressure to rotary actuator. The standard four-way directional valve controls the direction of the hydraulic fluid flow to the rotary actuator. In Figure 1, the hydrostatic transmission load that is moved by the actuator is shown as a rotary mass-spring-damper system with a load disturbance torque given by T_d. The mass moment of inertia, torsional spring rate, and the damping coefficient of the viscous for the load are shown in Figure 1 by the symbols (J), (b), and (k) respectively.

The rotary actuator is shown with the fixed volumetric displacement per unit of rotation V_a and

is connected to the rotating mass at the output shaft. In Figure 1, the inlet-throttled pump is used to design an angular velocity control system because the flow in the proposed system is adjusted by a valve positioned at the pump inlet to reduce the energy losses across the valve, where shows fixed-displacement pump is sized according to its volumetric displacement V_P and is driven by an external power source (not shown in Figure 1 at angular velocity ω_p. The pressure in the supply line of the charge pump is controlled using a high-pressure relief valve that is set at the desired supply pressure P_{in}. The charge pump itself is a fixed-displacement pump (usually a gear pump or a gerotor pump) that is used in conjunction with a relief valve for the purposes of providing makeup flow to the main fixed-displacement pump. The flow passages exist inherently within the system may also be designed for the purposes of directing fluid flow into the reservoir for cooling and filtration. The Coolers and filters are not shown in Figure 1.

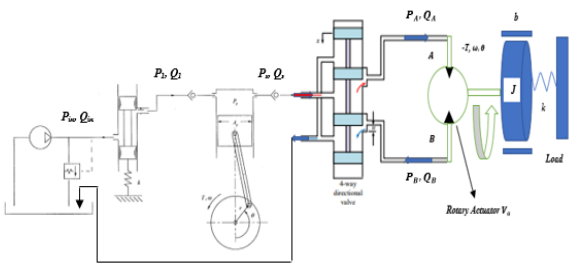

Figure 1: Angular Velocity Control System for a Rotary Actuator

3. Dynamic Model of the System

The Dynamic Model of the System response will be created in order to realize the dynamic problems, so a mathematical model should be written for the system. The Basic components for model system are shown in Figure 1. The mathematical equations of the plant system are derived. They include the torque dynamics as the rotary actuator's motion equation and pressure dynamics as the rate of pressure rise equation. The model has one inputs (A_v) and one disturbance (T_d).

The torque dynamics can be expressed as follows [14,15]:

$$J\ddot{\theta} + b\dot{\theta} + k\theta = \eta_{at}V_a(P_A - P_B) - T_d \quad (1)$$

In Eq. (6), the torque exerted on the load by the rotary actuator is given by $\eta_{at}V_a(P_A - P_B)$ where η_{at} is the torque efficiency of the actuator. The load spring is typically excluded from velocity control analysis, i.e., $k = 0$. $\dot{\theta} = \omega$ and $P_s = P_A$ then Eq. (1) becomes as Eq. (2):

$$J\ddot{\theta} + b\dot{\theta} = \eta_{at}P_sV_a - T_d \quad (2)$$

The rate of pressure rise equation can be expressed as follows:

$$\frac{V}{\beta}\dot{P}_s + k_1P_s = (Q_i - V_a\dot{\theta}) \quad (3)$$

The instantaneous volume of the chamber can be expressed as follows:

$$V = V_O + V_a\hat{\theta} \quad (4)$$

Also, $\hat{\theta}$ is considered here as the rotor rotation, therefore it can be expressed as follows:

$$\hat{\theta} = 2\pi(1 - \cos(\theta))/2 \quad (5)$$

where the inlet flow, Q_{in}, can be expressed as follows:

$$Q_i = A_vC_d\sqrt{\frac{2P_i}{\rho}} \quad (6)$$

Therefore, equation (7), accordingly, becomes as follows,

$$\dot{P}_s = \frac{\beta}{V_O+V_a\hat{\theta}}\left(A_vC_d\sqrt{\frac{2P_i}{\rho}} - k_1P_s - V_a\dot{\theta}\right) \quad (7)$$

The transfer function for the dynamics of the inlet throttled valve was experimentally determined and is shown in Eq. (8) [16]:

$$G_v(s) = \frac{A_v}{V_{in}} = \frac{k_vk_se^{-s\tau_d}\omega_n^2}{s^2+2\xi\omega_ns+\omega_n^2} \quad (8)$$

The time delay introduces a serious limitation on the controller performance that can be achieved. The reason for that limitation is that the effect of the change of the input on the output will be delayed by an amount of time that is equal to the time delay. The time delay limits the closed-loop bandwidth frequency to be less than the reciprocal of the time delay as shown in Eq. (9) [17]:

$$\omega_b < \frac{1}{\tau_d} \quad (9)$$

Now, the mathematical model of the inlet-throttled angular velocity control for rotary actuator system, transformed into state space form as follows:

$$\dot{\theta} = \omega \quad (10)$$

$$\dot{\omega} = -\frac{b}{J}\omega + \frac{\eta_{at}V_a}{J}P_s - \frac{T_d}{J} \quad (11)$$

$$\dot{P}_s = \frac{\beta}{V_O+V_a\hat{\theta}}\left(A_vC_d\sqrt{\frac{2P_i}{\rho}} - V_a\omega - k_1P_s\right) \quad (12)$$

From Eq. (8), the second derivative of the valve opening area can be written as:

$$\ddot{A}_v = -2\xi\omega_n\dot{A}_v - \omega_n^2A_v + k_vk_s\omega_n^2V_{in}(t-\tau_d) \quad (13)$$

The dynamic delay in $V_{in}(t-\tau_d)$ will be represented as a low pass filter

$$\frac{V_{in}(t-\tau_d)}{V_{in}(s)} = e^{-s\tau_d} = \frac{1}{\tau_d s+1} \quad (14)$$

or

$$\tau_d \dot{V}_{in}(t-\tau_d) + V_{in}(t-\tau_d) = V_{in}(t) \quad (15)$$

For the convenience of controller design, the following state variables are defined:

$$[\theta \;\; \dot{\theta} \;\; P_s \;\; A_v \;\; \dot{A}_v \;\; V_{in}(t-\tau_d)]^T \rightarrow [x_1 \;\; x_2 \;\; x_3 \;\; x_4 \;\; x_5 \;\; x_6]^T$$

Valve input voltage V_{in} was considered here as the control input. So, set $V_{in} = u$, but $\boldsymbol{x_6}$ is considered as the new control signal, where this the actual control signal is the input voltage with delay time. The state space model with a control signal $\boldsymbol{x_6}$ will be more appropriate for designing a controller, as well as we can consider $\hat{\theta} = \hat{x}_1$, $d = -\frac{T_d}{J}$, thus then we can write complete the mathematical model as follows:

For the system model dynamic without inlet throttling valve dynamic,

$$\left.\begin{aligned} \dot{x}_1 &= x_2 \\ \dot{x}_2 &= -a_1 x_2 + a_2 x_3 + d \\ \dot{x}_3 &= -b_1 x_2 - b_2 x_3 + c x_4 \end{aligned}\right\} \quad (16\text{-a})$$

And for the inlet throttling valve dynamic,

$$\left.\begin{aligned} \dot{x}_4 &= x_5 \\ \dot{x}_5 &= -\omega_n^2 x_4 - 2\xi\omega_n x_5 + k_v k_s \omega_n^2 x_6 \\ \dot{x}_6 &= -\frac{x_6}{\tau_d} + \frac{V_{in}(t)}{\tau_d} \end{aligned}\right\} \quad (16\text{-b})$$

4. Second-order Sliding Mode Control and Backstepping

Second-order sliding mode control is a powerful nonlinear control technique that offers significant advantages, particularly for systems with uncertainties and disturbances. It aims to drive the system state to zero in finite time, while ensuring robustness and stability. The second-order and higher-order sliding mode approaches have been actively developed over the last two decades for chattering attenuation and robust control of uncertain systems with relative degree two and higher respectively. The second-order sliding mode control, compared to first-order SMC has the advantage that it provides a smooth control and better performance in the control implementation yielding less chattering and better convergence accuracy while preserving the robustness properties.

The main idea is to reduce to zero, not only the sliding surface, but also its second-order derivative. It means that the second-order sliding mode corresponds to the control acting on the second derivative of the sliding surface [18]. It should be noted there are different types of 2-SMC algorithms such as the quasi-continuous 'twisting' and 'super-twisting', 'sub-optimal' and 'global', asymptotic observer algorithms, and drift algorithm. The paper referred about two proposed methods quasi-continuous and twisting algorithms. They can guarantee limited performances and robustness of the control system and the design procedure is usually not systematic, hence in complex systems it can be difficult to be applied. On the other hand, model-based control design is systematic and can be applied in general cases, and specifications in terms of robustness and tracking accuracy can be a priori assigned, as well as various criteria can be fulfilled [19]. Once more consider a dynamic system of the form:

$$\dot{x} = a(t,x) + b(t,x)u, \quad \sigma = \sigma(t,x) \quad (17)$$

u is control, σ is the only measured output with relative degree equal to two and the smooth functions a; b; are unknown. The task is to make the output σ vanish in finite time and to keep $\sigma \equiv 0$ by means of discontinuous globally bounded feedback control. The system trajectories are supposed to be infinitely extendible in time for any bounded input.

Assume that the measured output σ is twice differentiable with respect to time. Then calculating the second total time derivative $\ddot{\sigma}$ along the trajectories of Eq.(18), as shown in Eq. (19):

$$\ddot{\sigma} = h(t,x) + g(t,x)u \quad (18)$$

where the functions $h = \ddot{\sigma}\,|_{u=0}$, $g = \frac{\partial \ddot{\sigma}}{\partial u} \neq 0$ are some unknown smooth functions. Suppose that the inequalities:

$$0 < K_m \leq g \leq K_M, \;\; |h| < C. \quad (19)$$

hold globally for some $K_m; K_M$ and $C > 0$. Note that, at least locally, Eq. (19) is satisfied for any smooth system Eq. (18) with the well-defined relative degree 2. Obviously, no continuous feedback controller of the form $u = \varphi(\sigma, \dot{\sigma})$ can solve the stated problem. Indeed, such a control ensuring $\sigma \equiv 0$ has to satisfy the equality $\dot{\sigma} \equiv 0$ as well, which means that $\varphi(0,0) = -h(t,x)/g(t,x)$, whenever $\sigma \equiv \dot{\sigma} \equiv 0$. In other words, due to the uncertainty, the 2-sliding mode $\sigma \equiv \dot{\sigma} \equiv 0$ needs to be established. Assume now that Eq. (19) holds globally. Then Eqs. (18) and (19) imply the differential inclusion

$$\ddot{\sigma} \in [-C, C] + [K_m, K_M]u \quad (20)$$

Most 2-sliding controllers may be considered as controllers for Eq. (20) steering σ; $\dot{\sigma}$ to 0 in (preferably) finite time. Since the inclusion Eq. (20) does not "remember" the original system Eq. (17), such controllers are obviously robust with respect to any perturbations preserving Eq. (19). The problem is to find a feedback:

$$u = \varphi(\sigma, \dot{\sigma}) \quad (21)$$

such that all the trajectories of Eqs. (20) and (21) converge in finite time to the origin $\sigma \equiv \dot{\sigma} \equiv 0$ of the phase plane $\sigma, \dot{\sigma}$. We will now consider a number of the most popular controllers solving this problem. The controller guarantees the appearance of a 2-sliding mode $\sigma = \dot{\sigma}$ attracting the trajectories of the sliding variable dynamics in finite time [20].

Since the system relative degree with respect to σ is two while the system dimension when considering the valve dynamics is five, then we need to use the Backstepping control to design the actual control input voltage. Backstepping works its way recursively from the inner states (closest to the control input) to the outer states (system output). At the lower-level subsystem, it treats a specific state as a virtual control to design a control law. This virtual control helps achieve the desired behavior for the overall system.

Backstepping approach will enable us construction a sliding variable, which it is one of the two steps in designing a SOSMC. The Backstepping ensures also the asymptotic stability or at least the ultimate bound on the steady state error for the objective variable of lower-level subsystem. While deriving the control law (the second SMC design step) is made easily will ensure the attractiveness of the sliding manifold (the zero level of the sliding variable) [21].

5. Control Design and Stability Analysis

The second order sliding mode control (SOSMC) method is recognized as one efficient tool to design a robust controller for complex high-order nonlinear dynamical systems because it has superb characteristics such as insensitivity to large parameter variations; it's operating with the presence of disturbance inputs, and its ability to reject it. These characteristics gained SOSMC significant interest in recent years and made it a more attractive control method. Unfortunately, this control method has also a phenomenon namely the chattering effect, which may cause a glitch to system components in practical engineering systems.

However, many efforts have been made to minimize the chattering phenomenon. As well as this method is still being developed and implemented in many practical applications such as an underwater vehicle, a steered-by-wire road vehicle [22]. In this section, a convenience strategy to design a second order sliding mode controller will be presented. Firstly, we will divide the system in Eq.(16-a) and Eq.(16-b) into two subsystems; upper and lower subsystems. For lower-level subsystem, the sliding variable is assigned based on the standard or 1st order SMC theory. The objective from the designed controller is to force state trajectories into the level zero for each sliding variable. The loci of the points of the sliding variable level zero are called the sliding manifold or switching surface. After designing the SOSMC successfully, the state trajectory is directed towards the sliding manifold and then maintained it on this manifold for all future time. As a result, the state moves toward the origin or its neighborhood and stays there for all next time. This behavior is known as the reaching and sliding phases [23,24].

The uncertainty in the above equations (16-a) consists in the stiffness value; i.e., β and C_d can be written as:

Let $a_1 = \frac{b}{J}$, $a_2 = \frac{\eta_{at} V_a}{J}$, $b_1 = \frac{\beta V_a}{V_O + V_a \hat{x}_1}$, $b_2 = \frac{\beta k_1}{V_O + V_a \hat{x}_1}$ and $c = \frac{\beta C_d \sqrt{\frac{2P_i}{\rho}}}{V_O + V_a \hat{x}_1}$, then for $\beta = \beta_n + \Delta\beta$ and $C_d = C_{d_n} + \Delta C_d$ $\Longrightarrow b_1 = b_{1n} + \Delta b_1$, $b_2 = b_{2n} + \Delta b_2$ and $c_1 = c_n + \Delta c_1$.

Accordingly, the above equations (16-a) can be expressed as follows:

$$\left.\begin{aligned} \dot{x}_1 &= x_2 \\ \dot{x}_2 &= -a_1 x_2 + a_2 x_3 + d \\ \dot{x}_3 &= -b_{1n} x_2 - b_{2n} x_3 + c_n x_4 + \delta_1 \end{aligned}\right\} \quad (22)$$

where $\delta_1 = -\Delta b_1 x_2 - \Delta b_2 x_3 + \Delta c x_4$.

Note that in Eq. (22) the subscription refers to the functions with nominal parameters, d and δ_1, are the disturbance and perturbation terms, which they act on the dynamics of the system model. The first and the second subsystems are referred to them here as the upper and lower subsystems respectively. The system was modeled with two degrees of freedom but actuated by only one control input (the valve input voltage), i.e. the control input does not exist in the upper subsystem dynamics (the system model without inlet throttled valve dynamic model), which is affected by the perturbation δ_1, however; the control input does exist in the lower subsystem dynamics, in the inlet throttled valve dynamic model) which is affected by the perturbation δ_2 and δ_3. In this work, a nonlinear controller will be designed using the second order sliding mode control theory. The sliding mode control will be designed for each degree of freedom separately with the considering of a perturbation term δ_1 ,δ_2 and δ_3. Then using the Back-stepping approach, the control law can be derived. The proposed controller will enforce a desired behavior

on the overall system. Using the Back-stepping approach will enable one control action from controlling the system. As mentioned above, the SMC is designed for each subsystem; So, for the second line in Eq.(16-a), $\dot{x}_2 = -a_1 x_2 + a_2 x_3 + d$

So a sliding variable is defined according σ

$$\sigma = x_2 - x_{2d} \tag{23}$$

where σ is initially equal to zero. The first and second time rate of change of σ are given by

$$\dot{\sigma} = -a_1 x_2 + a_2 x_3 + d \tag{24}$$

$$\ddot{\sigma} = -a_1 \dot{x}_2 + a_2 \dot{x}_3 + \dot{d}$$
$$= -a_1(-a_1 x_2 + a_2 x_3 + d) + a_2(-b_1 x_2 - b_2 x_3 + c x_4) + \dot{d}$$
$$= (a_1^2 - a_2 b_1) x_2 - (a_1 a_2 + a_2 b_2) x_3 + a_2 c x_4 - a_1 d + \dot{d} \tag{25}$$

By considering x_4 as the virtual controller u_p, the $\ddot{\sigma}$ in the differential inclusion form is given by,

$$\ddot{\sigma} \in [-C, C] + [K_m, K_M] x_4$$

C can be selected according for the Eq.(25), in the following form in Eq.(20),

$$\left|(a_1^2 - a_2 b_1) x_2 - (a_1 a_2 + a_2 b_2) x_3 - a_1 d + \dot{d}\right| \leq |a_1^2 - a_2 b_1|_{max} |x_2| + |(a_1 a_2 + a_2 b_2)|_{max} |x_3| + \left|-a_1 d + \dot{d}\right|_{max} < C$$

while K_m and K_M is determined according $K_m \leq |a_2 c| \leq K_M$ where $K_m \leq |a_2 c| \leq K_M$, where $K_m \leq |a_2 c|_{min}$ and $|a_2 c|_{max} = K_M$.

Case 1: Twisting Controller

The twisting controller described below is the first 2-sliding controller which was proposed. It is defined by the formula:

$$u_p = -H_T * \left(r_1 sign(\sigma) + r_2 sign(\dot{\sigma})\right), \; r_1 > r_2 > 0 \tag{26}$$

where r_1 and r_2 satisfy the conditions

$$(r_1 + r_2) K_m - C > (r_1 - r_2) K_M + C, \quad (r_1 - r_2) K_m > C \tag{27}$$

$$H_T(t, \lambda_T) = \lambda_T * (1 - e^{-\alpha_T * t}) \tag{28}$$

where λ_T and α_T are positive constants which will be selected according to the required system response performance.

Case 2: Quasi-Continuous Controller

The controller in Eq. (29) guarantees the appearance of a 2-sliding mode $\sigma = 0$ and $\dot{\sigma} = 0$ attracting the trajectories of the sliding variable dynamics Eq. (23) in finite time.

An important class of controllers comprises the recently proposed so-called quasi- continuous controllers, featuring control continuous everywhere except the 2-sliding manifold $\sigma \equiv \dot{\sigma} \equiv 0$ itself. Since the 2-sliding condition requires the simultaneous fulfillment of two exact equalities, in the presence of any small noises and disturbances, the general-case trajectory does not ever hit the 2-sliding set. Hence, in practice the condition $\sigma \equiv \dot{\sigma} \equiv 0$ is never fulfilled, and the control remains continuous function of time, all the time. The larger the noises and switching imperfections, the worse the accuracy and the slower the changing rate of u_p. As a result, chattering is significantly reduced. The following is a 2-sliding controller with such features:

$$u_p = -\alpha \frac{\dot{\sigma} + \beta |\sigma|^{1/2} sign(\sigma)}{|\dot{\sigma}| + \beta |\sigma|^{1/2}} \tag{29}$$

This control is continuous everywhere except the origin and it vanishes on the parabola $\dot{\sigma} + \beta |\sigma|^{1/2} sign(\sigma) = 0$. For sufficiently large, there are numbers ρ_1; $\rho_2 : 0 < \rho_1 < \beta < \rho_2$ such that all the trajectories enter the region between the curves $\dot{\sigma} + \rho_i |\sigma|^{1/2} sign(\sigma) = 0$. $i = 1,2$ and cannot leave it, where:

$$\alpha, \; \beta > 0, \; \alpha K_m - C > 0 \tag{30}$$

Suppose the inequality

$$\alpha K_m - C - 2\alpha K_m \frac{\beta}{\rho + \beta} - \frac{1}{2}\rho^2 > 0 \tag{31}$$

holds for some positive $\rho > \beta$ (it is always true for a sufficiently large α), then the controller in Eq. (29) guarantees the establishment of a stable 2-sliding mode $\sigma \equiv 0$ for the sliding variable dynamics given by Eq. (23), in finite time.

$$H_Q(t, \lambda_Q) = \lambda_Q * (1 - e^{-\alpha_Q * t}) \tag{32}$$

where λ_Q and α_Q are positive constants which will be selected according to the required system response performance.

As we mentioned above, u_p is considered as the virtual control for the system dynamic which is given by Eq. (16-a). To derive the actual control system signal, the throttling valve dynamic is included Eq. (16-b), and we need again to rewrite it considering the nominal and the perturbation terms [25].

The uncertainty in Eq. (16-b) consists in the stiffness value too; i.e., ξ, ω_n, k_s and τ_d can be written as:

$\xi = \xi_n + \Delta\xi$, $\omega_n = \omega_{n_n} + \Delta\omega_n$, $k_s = k_{s_n} + \Delta k_s$ and $\tau_d = \tau_{d_n} + \Delta\tau_d$

So, Eq. (16-b) can be expressed as follows:

$$\left.\begin{aligned} \dot{x}_4 &= x_5 \\ \dot{x}_5 &= -2\xi_n\omega_{n_n}x_5 - \omega_{n_n}^2 x_4 + k_{v_n}k_{s_n}\omega_{n_n}^2 x_6 + \delta_2 \\ \dot{x}_6 &= -\frac{x_6}{\tau_{d_n}} + \frac{V_{in}(t)}{\tau_{d_n}} + \delta_3 \end{aligned}\right\} \quad (33)$$

where $\delta_2 = -2\Delta(\xi\omega_n)x_2 - \Delta\omega_n^2 x_4 + k_v\Delta(k_s\omega_n^2)x_6$ and $\delta_3 = -\Delta\left(\frac{1}{\tau_d}\right)x_6 + \Delta\left(\frac{1}{\tau_d}\right)V_{in}(t)$.

Note that in Eq. (33), the subscription refers to the functions with nominal parameters, δ_2, δ_3 are the perturbation terms, which they act on the second is the valve dynamic model respectively. the second subsystems are referred to them here as the lower subsystems respectively. The control input does exist in the lower subsystem dynamics, in the inlet throttled valve dynamic model, which is affected by the perturbation δ_2, δ_3.

In a similar way, the following steps are adapted for the lower subsystem which it given in Eq. (34). Let e_v be defined as:

$$e_v = x_4 - u_p \quad (34)$$

And it's the time rate of change is given by

$$\dot{e}_v = \dot{x}_4 - \dot{u}_p \quad (35)$$

As can be seen that the relative degree between s_v and the valve input voltage V_{in} is two, where V_{in} does not appear in x_5 control.

Accordingly, we must define the following sliding variable as an output with relative degree one can be defined as:

$$s = \dot{e}_v + \lambda_v e_v \quad (36)$$

And the time rate of change of s is:

$$\dot{s} = -2\xi_n\omega_{n_n}x_5 - \omega_{n_n}^2 x_4 + k_{v_n}k_{s_n}\omega_{n_n}^2 x_6 + \delta_2 - \ddot{u}_p + \lambda_v\dot{e}_v \quad (37)$$

where δ_2 is perturbation and $\lambda_v > 0$ is a design parameter. To evaluate $\dot{e}_v$ we need to determine the time rate of change of u_p, and since $\dot{u}_p$ is uncertain, therefore we need to estimate it through the sliding mode observer in Appendix (A) [26,27].

Again, consider x_6 be the virtual controller and denote it by u_v. Then to design the control u_v , we use the following non-smooth Lyapunov function:

$$V = \frac{1}{2}s^2 \quad (38)$$

To ensure the attractiveness of the sliding manifold ($s = 0$), k_v is selected such that the derivative of the Lyapunov function V_v is negative definite as can be shown in the following steps;

$$\left.\begin{aligned} \dot{V}_v &= sgn(s) * \dot{s} \\ &= sgn(s) * \left[-\omega_{n_n}^2 x_4 - 2\xi_n\omega_{n_n}x_5 + k_{v_n}k_{s_n}\omega_{n_n}^2 u_v + \delta_2 - \ddot{u}_p + \lambda_v\dot{e}_v\right] \\ &= s * \left[-\omega_{n_n}^2 x_4 - 2\xi_n\omega_{n_n}x_5 + k_{v_n}k_{s_n}\omega_{n_n}^2 u_v + \hat{\delta}_2\right] \end{aligned}\right\} \quad (39)$$

where $\hat{\delta}_2 = \delta_2 - \ddot{u}_p + \lambda_v\dot{e}_v$.

Now, let

$$u_v = (u_{vn} + u_{vs})/(k_{v_n}k_{s_n}\omega_{n_n}^2) \quad (40)$$

Let the first term in the control law is u_{vn} is taken here as:

$$u_{vn} = \omega_{n_n}^2 x_4 + 2\xi_n\omega_{n_n}x_5 \quad (41)$$

While the second term in the control law is u_{vs} is taken as:

$$u_{vs} = -k_v * H_v(t) * s \quad (42)$$

Here the $H_v(t)$ function is a positive function defined as

$$H_v(t) = (1 - e^{-\alpha_v * t}) \quad (43)$$

where α_v is positive constant which will be selected according to the required system response performance. Accordingly, $\dot{V}_v$ becomes;

$$\left.\begin{aligned} \dot{V}_v &= s * \left[-k_v * H_v(t) * s + \hat{\delta}_2\right] \\ &\le -k_v * H_v(t) * s^2 + |s||\hat{\delta}_2| \\ &\le -(1-\beta_2)k_v * H_v(t) * s^2, \ \forall |s| > \frac{|\hat{\delta}_2|}{k_v H_v(t)\beta_2} \ \ 0 < \beta_2 < 0 \end{aligned}\right\} \quad (44)$$

Again, as in the previous design steps, s is ultimately bounded by $b_v = \frac{|\hat{\delta}_2|}{\beta_2 k_v H_v(t)}$.

Not that, the actual control input voltage $V_{in}(t)$ can be taken equal to the designed controller u_v and study the effect of the delay in the valve system dynamic through the simulations and in this case the virtual controller x_6 will take a period of time to follow the designed controller u_v . one can reduce the delay time effect via modifying the relation between $V_{in}(t)$ and u_v in the following form

$$V_{in}(t) = x_6\left\{1 - \frac{\tau_{d_n}}{\hat{\tau}_{d_n}}\right\} + \frac{\tau_{d_n}}{\hat{\tau}_{d_n}}u_v \quad (45)$$

where $\hat{\tau}_{d_n}$ is a design parameter.

Now we need to explore how the ultimate bounds b_v and b_p affected the main design objective which it is the ultimate bound b_e on the error function e. The following proposition give the answer about this question.

Appendix (A)

In order to estimate $\dot{u}_p$ (assuming a bound on $|\dot{u}_p|$ is known) the following observation algorithm is proposed:

$$\dot{x}_7 = \dot{u}_p \quad (46)$$

where y_1 is an observer injection term that is to be designed so that the estimates $x_7, \dot{x}_7 \to u_p, \dot{u}_p$. Let us introduce an estimation error (an auxiliary sliding variable):

$$y_1 = u_p - x_7 \quad (47)$$

$$\dot{y}_1 = \dot{u}_p - \dot{x}_7 \quad (48)$$

Let $u_p(0) = x_7(0)$ and make the injection term x_7 that drives $y_1 = u_p - x_7 \to 0$ in finite time.

In this case x_7 will converge to u_p in finite time. Let the following choice of injection term:

$$\dot{x}_7 = \left(1 - exp(-\alpha_2 * t)\right) * ku * y_1 \quad (49)$$

$\alpha_2 > 0$, $ku > 0$ and $u_p \to 0$, or $x_7 \to u_p$. The sliding mode dynamics are computed using the concept of equivalent control [26]:

$$\dot{y}_1 = \dot{u}_p - \dot{x}_7 = 0 \quad (50)$$

It is clear that the state variable $\dot{u}_p$ can be exactly estimated as:

$$\dot{u}_p = \dot{x}_7, t \geq t_r \quad (51)$$

6. Results and Discussion

The dominant parameters in the system model of the proposed hydrostatic transmission (HST) systems are given in Table 2, which presents the values of the system model parameters.

Table 2: Model Parameters

Dimensional Quantity	Definition	The value (SI units)
k_s	static gain of the valve	0.72
k_1	Leakage Coefficient	$0.14*10^{-11}\ m^4.s/kg$
k_v	constant of proportionality	$3.75*10^{-6}\ m^2/volt$
P_s	Pressure Supply	$25*10^6\ N/m^2$
cd	Discharge Coefficient	0.62
P_i	input pressure	$2*10^6\ N/m^2$
V_o	Actuator Volume	$8.2*10^{-6}\ m^3$
J	Mass moment of inertia	$0.013\ kg.m^2$
ρ	fluid density	$850\ kg/m^3$
b	viscous damping coefficient	$0.025065\ kg.m^2/s$
V_a	Volumetric displacement of the actuator	$1.3051*10^6\ m^3/rad$
β	Fluid Bulk Modulus	$1*10^9\ N/m^2$
η_{at}	Actuator mechanical Efficiency	0.95
ω_n	Valve Natural Frequency	$85\ rad/s$
τ_d	time delay of valve	0.015 s
ξ	Damping Ratio of the Valve	0.8

The parameters in the robust controller are given in Table 3, which presents the values of the controller parameters.

Table 3: The Definitions of Quantities of Controller

Parameters	Value	Model Type
C	25	Control low of upper- level Subsystem (Twisting Controller)
r_1	24.1	
r_2	14.4613	
K_M	5.1867	
K_m	2.5933	
λ_T	4.5	
α_T	0.5	
C	25	Control low of upper-level subsystem (Quasi-Continuous Controller)
α	9.6402	
ρ	1	
β	0.01	
K_m	2.5933	
λ_Q	18	
α_Q	0.5	
λ_v	0.4	Control low of lower-level subsystem
α_1	2	
k_v	$5 * 10^{-3}$	
ku	100	Estimator
α_2	0.5	

The parameters of the switching function in Eq.(23) and switching function in Eq.(36) are chosen depending on table (3). The reduced dynamics, when the states reach zero value in a finite time, is exponentially asymptotically stable. In deriving the sliding mode control laws in Eqs. (26) and (29) for each controller respectively for the upper-level subsystem and Eq. (40) for the lower-level subsystem, where the nominal system parameters are considered as well as the disturbances and uncertainties. The sliding mode controller will definitely overcome system uncertainties for suitable control laws. This design chose the desired velocity as $1600\ RPM$ at zero second with disturbance torque $25\ N.m$, was applied to the actuator, as an external load at 35 seconds, where the effects of the disturbance torque on the angular velocity ω_a, desired pressure P_s, valve opening area A_V, input voltage V_{in}, are shown in the Figures (2-18) for three cases as followed:

Case1: Constant desired angular velocity

The desired angular velocity of actuator to $x_{2d} = 1600\ \text{RPM} \rightarrow 167.5516\ \text{rad/s}$ is supplied as a set point. As a result, the angular velocity reaches the final value at steady state for the two robust controllers with the supplied disturbance torque effects $(25\ N.m)$ is applied in the time = 35 sec at steady state with high stability and performance as shown in Figure 2. The response results of the robust controller are shown in Table 4.

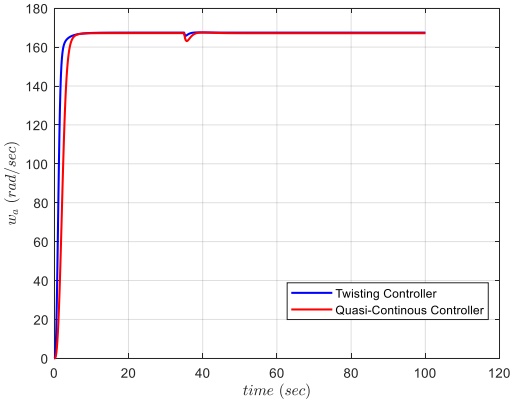

Figure 2: The velocity time response of closed-loop with two robust controllers with torque disturbances effects

Table 4: Results of velocity time response with two robust controllers

Robust Controllers	TC	QCC
Steady state value	167.4 rad /s	167.2 rad /sec
Error steady State	0.1516 rad/sec	0.3516 rad/sec
Rise Time	1.363 sec	2.45 sec
Max. Overshoot	0	0
Steady state value (with disturbance)	167.4 rad /s	167.1 rad /sec

The desired angular velocity of actuator to $x_{2d} = 1600\ \text{RPM} \rightarrow 167.5516\ \text{rad/s}$ is supplied as a set point. As a result, the pressure supply reaches the final value at steady state for the two robust controllers with the supplied disturbance torque $(25\ N.m)$ effects is applied in the time = 35 sec at steady state with high stability and performance as shown in Figure 3. The response results of the robust controller are shown in Table 5.

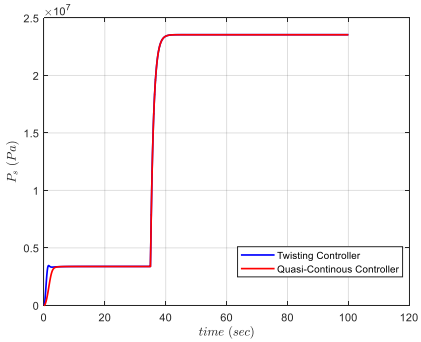

Figure 3: The pressure supply time response of closed-loop with two robust controllers with torque disturbances effects

Table 5: Results of pressure supply time response with two robust controllers

Robust Controllers	TC	QCC
Steady state value	3.385 MP	3.38 MP
Rise Time	1.335 sec	2.07sec
Max. Overshoot(%)	2.304 %	0
Steady state value (with disturbance)	23.55 MP	23.54 MP

The desired angular velocity of actuator to $x_{2d} = 1600\ \text{RPM} \rightarrow 167.5516\ \text{rad/s}$ is supplied as a set point. As a result, the valve opening area reaches the final value at steady state for the two robust controllers with the supplied disturbance torque $(25\ N.m)$ effects is applied in the time = 35 sec at steady state with high stability and performance as shown in Figure 4. The response results of the two robust controllers are shown in Table 6.

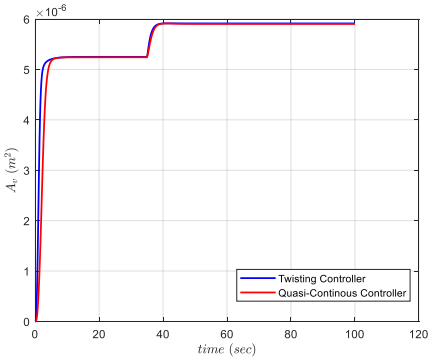

Figure 4: The valve opening area time response of closed-loop with two robust controllers with torque disturbances effects

Table 6: Results of valve opening area time response with two robust controllers

Robust Controllers	TC	QCC
Steady state value	$5.25 \times 10^{-6}\ m^2$	$5.241 \times 10^{-6}\ m^2$
Rise Time	1.393 sec	2.49 sec
Max.Overshoot (%)	0	0
Steady state value (with disturbance)	$5.913 \times 10^{-6}\ m^2$	$5.904 \times 10^{-6}\ m^2$

The desired angular velocity of actuator to $x_{2d} = 1600\ \text{RPM} \rightarrow 167.5516\ \text{rad/s}$ is supplied as a set point. As a result, the control action (V_{in} with delay time) reaches the final value at steady state for the two robust controllers with the supplied disturbance torque $(25\ N.m)$ effects is applied in the time = 35 sec at steady state with high stability and performance as shown in Figure 5. The response results of the robust controller are shown in Table 7.

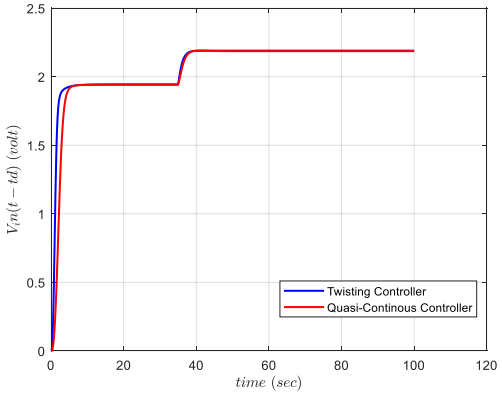

Figure 5: The control action time response of closed-loop with two robust controllers with torque disturbances effects

Table 7: Results of valve opening area time response with two robust controllers

Robust Controllers	TC	QCC
Steady state value	1.944 volt	1.941 volt
Rise Time	1.3715 sec	2.485 sec
Max.Overshoot (%)	0	0
Steady state value (with disturbance)	2.19 volt	2.186 volt

The desired angular velocity of actuator to $x_{2d} = 1600\ \text{RPM} \rightarrow 167.5516\ \text{rad/s}$ is supplied as a set point. As a result, the valve input voltage (V_{in}) reaches the final value at steady state for the two robust controllers with the supplied disturbance torque $(25\ N.m)$ effects is applied in the time = 35 sec at steady state with high stability and performance as shown in Figure 6. The response results of the robust controller are shown in Table 8.

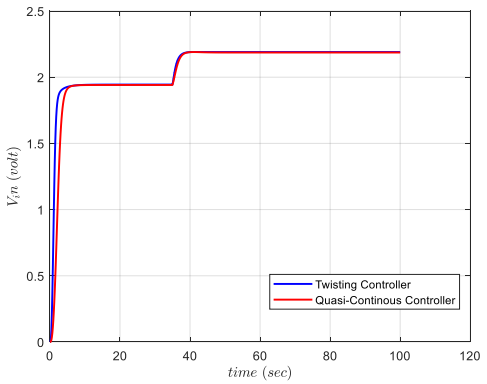

Figure 6: The valve input voltage time response of closed-loop with two robust controllers with torque disturbances effects

Table 8: Results of valve input voltage time response with two robust controllers

Robust Controllers	TC	QCC
Steady state value	1.944 volt	1.941 volt
Rise Time	1.3875	2.62 sec
Max.Overshoot (%)	0	0
Steady state value (with disturbance)	2.19 volt	2.186 volt

Case2: Piecewise constant desired angular velocity

At the time = 100 s, at steady state, this design chose increasing the set point with $x_{2d} = 36.6519\ \text{rad/s}$. As a result, the angular velocity reaches the final value at steady state for the two robust controllers but at the time = 200 s , at steady state, this design chose adjusting the set point with $x_{2d} = -20.944\ \text{rad/s}$. As a result, the angular velocity reaches another final value at steady state for the two robust controllers with high stability and performance as shown in Figure 7. This demonstrates that the proposed controller can meet various operational requirements. The response results of the robust controller are shown in Table 9.

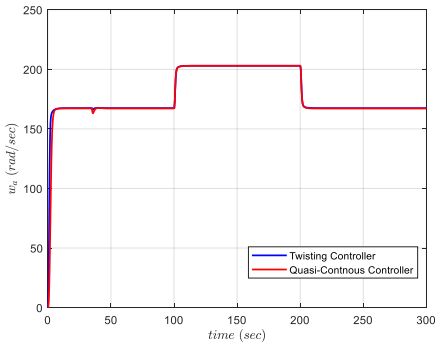

Figure 7: The velocity time response of multi steps for closed-loop with two robust controllers with torque disturbances

Table (9): Results of velocity time response of multi steps for two robust controllers

Robust Controllers	TC	QCC
Steady state value with set point (167.5516 rad/sec)	167.4 rad/s	167.1 rad/sec
Steady state value with increasing set point (36.6519 rad/sec)	204 rad/sec	203.7 rad/sec
Error steady State with increasing set point (36.6519 rad/sec)	0.0519 rad/sec	0.0519 rad/sec
Steady state value with decreasing set point (−20.944 rad/sec)	182.1 rad/s	182.1 rad/s
Error steady State with decreasing set point (−20.944 rad/sec)	0.956 rad/sec	0.656 rad/sec

At the time = 100 s, at steady state, this design chose increasing the set point with $x_{2d} = 36.6519$ rad/s . As a result, the pressure supply reaches a final value at steady state for the two robust controllers but at the time = 200 s , at steady state, this design chose adjusting the set point with $x_{2d} = -20.944$ rad/s . As a result, the pressure supply reaches another final value at steady state for the two robust controllers with high stability and performance as shown in Figure 8. This demonstrates that the proposed controller can meet various operational requirements. The response results of the robust controller are shown in Table 10.

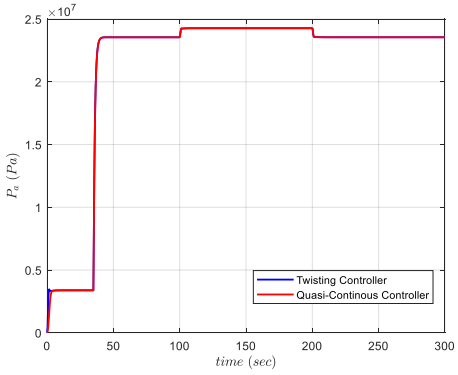

Figure 8: The pressure supply time response of multi steps for closed-loop with two robust controllers with torque disturbances

Table (10): Results pressure supply time response of multi steps for two robust controllers

Robust Controllers	TC (Case 1)	QCC
Steady state value with set point (167.5516 rad/sec)	23.55 MP	23.54 MP
Steady state value with increasing set point (36.6519 rad/sec)	24.29 MP	24.28 MP
Steady state value with decreasing set point (−20.944 rad/sec)	23.85 MP	23.85 MP

At the time = 100 s, at steady state, this design chose increasing the set point with $x_{2d} = 36.6519$ rad/s . As a result, the valve opening area reaches a final value at steady state for all the two robust controllers but at the time = 200 s , at steady state, this design chose adjusting the set point with $x_{2d} = -20.944$ rad/s . As a result, the valve opening area reaches another final value at steady state for the two robust controllers with high stability and performance as shown in Figure 9. This confirms that the proposed controllers can meet various operational requirements. The response results of the robust controller are shown in Table 11.

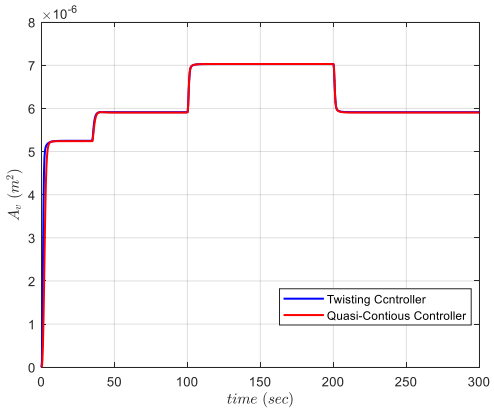

Figure 9: The valve opening area of multi steps for two robust controllers with torque disturbances effects

Table 11: Results of opening area time response of multi steps for two robust controllers

Robust Controllers	TC (Case 1)	QCC
Steady state value with set point (167.5516 rad/sec)	5.913×10^{-6}m^2	5.904×10^{-6}m^2
Steady state value with increasing set point (36.6519 rad/sec)	7.061×10^{-6}m^2	7.052×10^{-6}m^2
Steady state value with decreasing set point (−20.944 rad/sec)	6.372×10^{-6}m^2	6.373×10^{-6}m^2

At the time = 100 s, at steady state, this design chose increasing the set point with $x_{2d} = 36.6519$ rad/s . As a result, the control action reaches a final value at steady state for all the two robust controllers but at the time = 200 s , at steady state, this design chose adjusting the set point with $x_{2d} = -20.944$ rad/s . As a result, the valve opening area reaches another final value at steady state for the two robust controllers with high stability and performance as shown in Figure 10. This demonstrates that the proposed controller can meet various operational requirements. The response results of the robust controller are shown in Table 12.

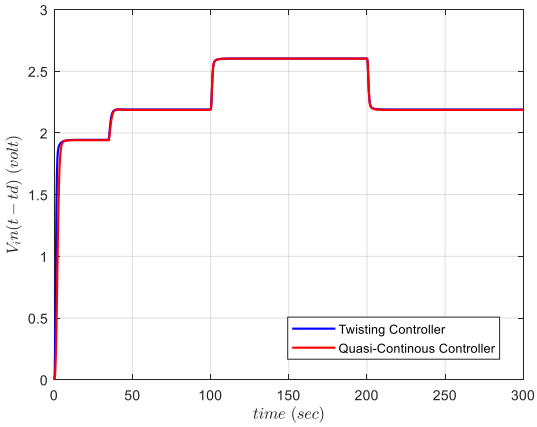

Figure 10: The control action time response of multi steps for two robust controllers with torque disturbances effects

Table 12: Results of multi steps control action time response of multi steps with two robust controllers

Robust Controllers	TC (Case 1)	QCC
Steady state value with set point (167.5516 rad /sec)	2.19 volt	2.186 volt
Steady state value with increasing set point (36.6519 rad/sec)	2.615 volt	2.611 volt
Steady state value with decreasing set point (−20.944 rad/sec)	2.36 volt	2.36 volt

Case3: Control robustness under parameters uncertainty

For the Backstepping Twisting Controller, Figures (11-14) show the time response of the uncertain system with multiplicative uncertainty within the range of ±10% of the nominal values for the six parameters of the system. It could be noticed that the system has good performance within the whole uncertainty set. Note that the responses stayed have high stability and performance although the high uncertainties.

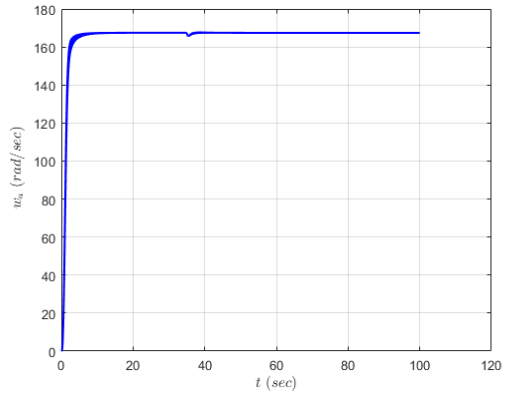

Figure 11: The perturbed velocity time response for closed-loop with (BTC) and disturbances effects

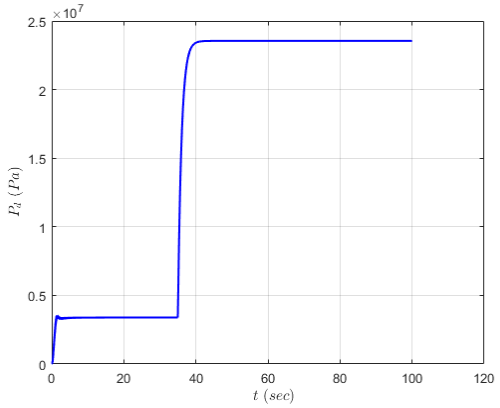

Fig. (12): The perturbed pressure supply time response for closed-loop with (BTC) and disturbances effects

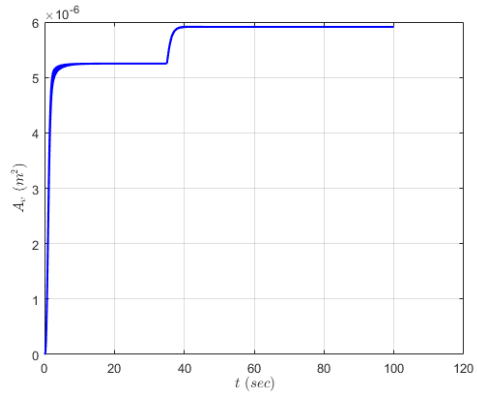

Figure 13: The perturbed valve opening area time response for closed-loop with (BTC) and disturbances effects

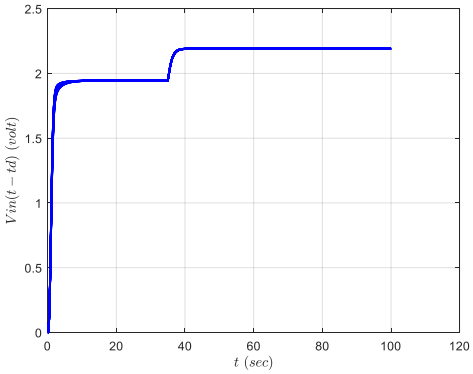

Figure 14: The perturbed control action time response for closed-loop with (BTC) and disturbances effects

For the Backstepping Quasi-Continuous Controller, Figures (15,16,17,18) show the time response of the uncertain system with multiplicative uncertainty. The uncertainties were determined based on errors in uncertain parameters of nominal system within the range of ±10% of the nominal values for the six parameters of the system. It could be noticed that the system has good performance within the whole uncertainty set. Note the responses stayed have high stability and performance although the high uncertainties.

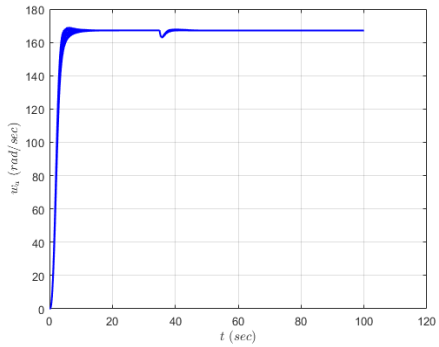

Figure 15: The perturbed velocity time response for closed-loop with (BQCC) and disturbances effects

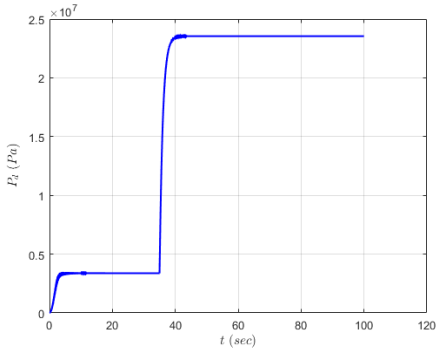

Figure 16: The perturbed pressure supply time response for closed-loop with (BQCC) and disturbances effects

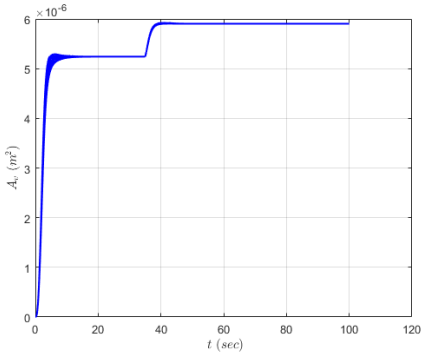

Figure 17: The perturbed valve opening area time response for closed-loop with (BQCC) and disturbances effects

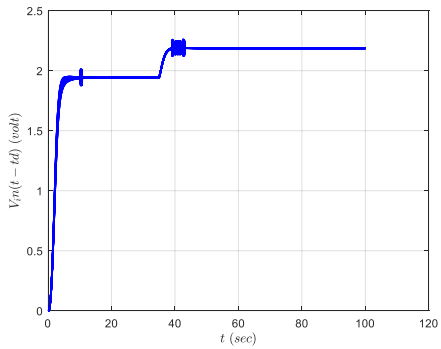

Fig. (18): The perturbed control action time response for closed-loop with (BQCC) and disturbances effects

7. Conclusions

This work presents a design of a Backstepping Quasi-Continuous and Backstepping Twisting Controllers for controlling the angular velocity of a rotary actuator. Two switching functions for two level subsystems; low level subsystem and high level subsystem have been constructed where the back-stepping method was used. The controlled system's stability analysis has been presented using the Lyapunov function in the low level subsystem. The second order control action is used for the high level subsystem and the conventional sliding mode is used for the low level subsystem. The simulation results demonstrated that the Backstepping Quasi-Continuous and Backstepping Twisting Controllers ensure robust stability and performance in the time-domain specifications with uncertainties and disturbances. It can be concluded from the inlet throttled system can be used as a great alternative for the available hydraulic power transmission (Pump controlled and valve controlled systems) if the right control technique is used. It can also be concluded that both the backstepping quasi-continuous and backstepping twisting controllers provide a precise control for the system. However, twisting controller provide beter performance in terms of response speed and disturbance rejection.

References

[1] Zhou Jing and Han Qi," Design and Calculation of Hydraulic Transmission System of Loader," MMEAT 2020 Journal of Physics: Conference Series 1676 (2020) 012242 IOP Publishing, doi:10.1088/1742-6596/1676/1/012242.

[2] Hasan H. Ali, and Roger C. Fales," A review of flow control methods," International Journal of Dynamics and Control (2021) 9:1847–1854 https://doi.org/10.1007/s40435-020-00730-y.

[3] Xinhao, Chengwen Wang, Zhenyang Zhang, Shuai Chen and Xinping Guo, "Nonlinear adaptive position control of hydraulic servo system based on sliding mode back-stepping design method", Proc IMechE Part I: J Systems and Control Engineering 1–12 © IMechE 2020 Article reuse guidelines: sagepub.com/journals-permissions DOI:10.1177/0959651820949663. journals.sagepub.com/home/pii.

[4] Yuri B. Shtessel, Jaime A. Moreno and Leonid M. Fridman, "Twisting sliding mode control with adaptation: Lyapunov design, methodology and application" in 2017 ELSEVER, A Journal IFAC - the International Federation of Automatic Control, pp.229–235, Jan. 2017. DOI: 10.1109/CINTI.2011.6108547.https://doi.org/10.1016/j.automatica.2016.09.004

[5] Jose Kochalummoottil, Yuri B. Shtessel, Jaime A. Moreno, and Leonid Fridman, "Output Feedback Adaptive Twisting Control: A Lyapunov Design" in 2012 American Control Conference Fairmont

Queen Elizabeth, Montréal, Canada June 27-June 29, 2012. DOI: 10.1109/ACC.2012.6315242.

[6] Tenoch Gonzalez, Leonid Fridman and Jaime A Moreno, "Variable Gain Super-Twisting Sliding Mode Control" in 2012 IEEE Transactions on Automatic Control, DOI: 10.1109/TAC.2011.2179878

[7] E. Bernuau, D. Efimov, W. Perruquetti, and A. Polyakov, "On homogeneity and its application in sliding mode control," Journal of the Franklin Institute, vol. 351, pp. 1866–1901, Apr. 2014. DOI: 10.1016/j.jfranklin.2014.01.007.

[8] L. Derafa, A. Benallegue, and L. Fridman, "Super twisting control algorithm for the attitude tracking of a four rotors UAV," Journal of the Franklin Institute, vol. 349, pp. 685–699, Mar. 2012. DOI: 10.1016/j.jfranklin.2011.10.011.

[9] S. Rajappa, C. Masone, H. H. Bülthoff, and P. Stegagno, "Adaptive Super Twisting Controller for a quadrotor UAV," in 2016 IEEE International Conference on Robotics and Automation (ICRA), pp. 2971–2977, May 2016. DOI:10.1109/ICRA.2016.7487462.

[10] E.-H. Zheng, J.-J. Xiong, and J.-L. Luo, "Second order sliding mode control for a quadrotor UAV," ISA Transactions, vol. 53, pp. 1350–1356, July 2014. DOI: 10.1016/j.isatra.2014.03.010.

[11] Benallegue, A. Mokhtari, and L. Fridman, "High-order sliding-mode observer for a quadrotor UAV," International Journal of Robust and Nonlinear Control, vol. 18, pp. 427–440, Mar. 2008. DOI: 10.1002/rnc.1225

[12] Y. Zhang and A. Chamseddine, "Fault Tolerant Flight Control Techniques with Application to a Quadrotor UAV Testbed,"2012. DOI: 10.5772/38918.

[13] H. Bouadi, S. S. Cunha, A. Drouin, and F. Mora-Camino, "Adaptive sliding mode control for quadrotor attitude stabilization and altitude tracking," in 2011 IEEE 12th International Symposium on Computational Intelligence and Informatics (CINTI), pp.449–455, Nov. 2011. DOI: 10.1109/CINTI.2011.6108547.

[14] [14] Yuri Shtessel Christopher Edwards Leonid Fridman and Arie Levant," Sliding Mode Control and Observation", ISBN 978-0-8176-4892-3 ISBN 978-0-8176-4893-0 (eBook), DOI 10.1007/978-0-8176-4893-0, Springer New York Heidelberg Dordrecht London Library of Congress Control Number: 2013934106, Mathematics Subject Classifications (2010): 93B12,93C10, 93B05, 93B07, 93B51, 93B52, 93D25

[15] Vadim Utkin • Alex Poznyak • Yury V. Orlov • Andrey Polyakov," Road Map for Sliding Mode Control Design", ISSN 2191-8198, ISSN 2191-8201 (electronic), SpringerBriefs in Mathematics, (2014), ISBN 978-3-030-41708-6, ISBN 978-3-030-41709-3 (eBook), https://doi.org/10.1007/978-3-030-41709-3

[16] Ahmed Khalaf Hamoudi and Luay Thamir Rasheed," Design and Implementation of Adaptive Backstepping Control for Position Control of Propeller-Driven Pendulum System", Journal Européen des Systèmes Automatisés, Vol. 56, No.2, April, 2023, pp. 281-289, Journal homepage: http://iieta.org/journals/jesa.

[17] Ali HH, Fales RC, Manring ND (2019) "Modeling and control design for an inlet metering valve-controlled pump that controls actuator velocity via H-infinity and two-degrees-of-freedom methods". https://doi.org/10.1115/1.4044182.

[18] Ali, Hasan H., Firas M. Abdulsattar, and Ahmed W. Mustafa. "A New Mechanical Analysis of a Crankshaft-connecting Rod Dynamics Using Lagrange's Trigonometric Identities." Journal of Engineering & Technological Sciences 54, no. 2 (2022).

[19] Humaidi, A.J., Hameed, M.R., Ajel, A.R., ...Al-Qassar, A.A., Ibraheem, I.K, "Block Backstepping Control Design of Two-Wheeled InvertedPendulum Via Zero Dynamic Analysis", 2021, IEEE 12th Control and System Graduate Research Colloquium, ICSGRC 2021- Proceedings, 2021, pp. 87–92.

[20] Abdul-Adheem, W.R., Alkhayyat, A., Mhdawi, A.K.A., ...Humaidi, A.J., Al-Qassar, A.A, "Anti-disturbance compensation-based nonlinear control for a class of MIMO uncertain nonlinear systems" Entropy, 2021, 23(11), 1487.

[21] HASSAN K. KHALIL," Nonlinear Systems Third Edition", © 2002, 1996 by Prentice Hall Prentice-Hall, Inc. Upper Saddle River, NJ 07458.

[22] Rasheed, L.T., Hamzah, M.K., "Design of an optimal backstepping controller for nonlinear system under disturbance", Engineering and Technology Journal, (2021), 39(3): 465-476.https://doi.org/10.30684/etj.v39i3A.1801

[23] Humaidi, A., Hameed, M. (2019). Development of a new adaptive backstepping control design for a nonstrict and under-actuated system based on a PSO tuner. MDPI, Information, 10(2): 38, pp. 1-17.https://doi.org/10.3390/info10020038

[24] Shibly Ahmed AL-Samarraie, Shaymaa Mahmood Mahdi, Taghreed M. Mohammad Ridha and Mustafa Hussein Mishary," Sliding Mode Control for Electro-Hydraulic Servo System", IJCCCE Vol.15, No.3, 2015

[25] Waheed, Z.A., Humaidi, A.J., Sadiq, M.E., ...Ajel, A.R., Abbas, S.J," CONTROL OF ELBOW REHABILITATION SYSTEM BASED ON OPTIMAL-TUNED BACKSTEPPING SLIDING MODE CONTROLLER", Journal of Engineering Science and Technology, 2023, 18(1), pp. 584–603.

[26] Ahmed Mohsen Mohammad, Shibly Ahmed AL-Samarraie," Robust Controller Design for Flexible Joint Based on Back-Stepping Approach", Iraqi Journal of Computer Communications, Control and Systems Engineering (IJCCCE), Vol. 20, No.2, April 2020.

[27] Al-Samarraie, S.A. (2013), "Invariant sets in sliding mode control theory with application to servo actuator system with Friction", WSEAS Transactions on Systems and Control, 8(2): 33-45.